

LASER BEAMS

https://doi.org/10.1070/QEL16457

Formation of doughnut and super-Gaussian intensity distributions of laser radiation in the far field using a bimorph mirror

A.N. Lylova, Yu.V. Sheldakova, A.V. Kudryashov, V.V. Samarkin

Abstract. **We consider the methods for modelling doughnut and super-Gaussian intensity distributions in the far field by means of deformable bimorph mirrors. A method for the rapid formation of a specified intensity distribution using a Shack–Hartmann sensor is proposed, and the results of the modelling of doughnut and super-Gaussian intensity distributions are presented.**

Keywords: *formation of a specified intensity distribution, adaptive optics, deformable mirror, Shack–Hartmann sensor.*

1. Introduction

Radiation with various shapes of focal spots is often used in the industry for laser cutting, laser heat treatment of surfaces, etc. Traditionally, the required intensity distributions are obtained by using complex optical elements and circuits [1, 2], diffraction optical devices [3] or kinoforms [4, 5]. The focal spot shapes obtained with the use of these methods have high quality and minimal laser intensity losses. However, a significant drawback of these approaches is the impossibility to change the required intensity distribution in real time in the process of work, which is necessary for the realisation of a correct technological process (for example, in microelectronics).

One of the solutions to this problem is the use of adaptive optics, which, as a rule, is used to improve the focusing of radiation transmitted through optically inhomogeneous media [6], but can also be used to form various intensity distributions in the far field [7].

The purpose of this paper is a search for such a way of determining and introducing a phase delay into the system (using an adaptive phase corrector) so that the resulting focal spot would as closely as possible correspond to a predetermined shape.

A scheme for the formation of a specified intensity distribution in the far field is shown in Fig. 1. When a laser beam falls onto a phase corrector, the wavefront changes in such a way that the intensity distribution closest to the required one would be obtained in the observation plane.

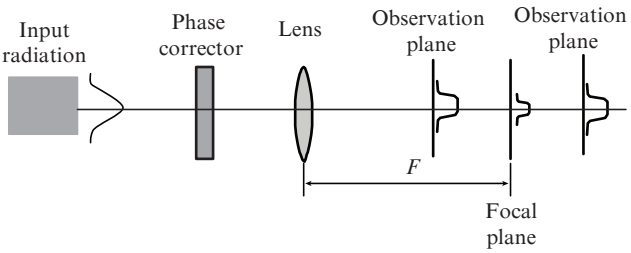

Figure 1. Scheme for the formation of a specified intensity distribution in the far field.

For a correct solution of the problem of the formation of a focal spot of required shape, use is made of iterative algorithms to optimise the output parameters of laser radiation (gradient methods [8], Newton's method [9], simplex method [9] and genetic algorithms [10]). However, such algorithms require a considerable number of iterations and a fairly long computation time (the process may take several tens of seconds), and consequently, they are unable to monitor dynamically the distortion of the laser beam wavefront and to respond quickly to the changes in the given intensity distribution. To overcome this problem, a system was proposed that implements the phase conjugation mechanism based on the use of a Shack–Hartmann wavefront sensor. This sensor makes it possible to measure the light radiation phase in real time [11–15]. The phase conjugation algorithm is widely used in laser systems for rapid correction of aberrations, though it can also be used to change the focal spot shape in a necessary manner [15]. In this paper we present the results of using this method in systems for generating the required intensity distribution in the far field.

In the approach proposed, the general statement of the problem was reduced to the determination of the radiation phase which is necessary to obtain a specified intensity distribution either in the lens focal plane or at some distance from it. In this case, as the initial data, the information about the intensity distribution in the observation plane was only used.

A.N. Lylova Institute of Geosphere Dynamics, Russian Academy of Sciences, Leninsky prosp. 38, korp. 1, 119334 Moscow, Russia; 'Active Optics NightN' Ltd, Sudostroitel'naya ul. 18, korp. 5, 115407 Moscow, Russia; e-mail: lylova@activeoptics.ru;
Yu.V. Sheldakova Institute of Geosphere Dynamics, Russian Academy of Sciences, Leninsky prosp. 38, korp. 1, 119334 Moscow, Russia;
A.V. Kudryashov, V.V. Samarkin Institute of Geosphere Dynamics, Russian Academy of Sciences, Leninsky prosp. 38, korp. 1, 119334 Moscow, Russia; Moscow Polytechnic University, Bol'shaya Semenovskaya ul. 38, 107023 Moscow, Russia;
e-mail: kud@activeoptics.ru

Received 25 June 2017; revision received 21 September 2017
Kvantovaya Elektronika **48** (1) 57–61 (2018)
Translated by M.A. Monastyrskiy

One of the ways to determine the phase delay in the formation of a specified intensity distribution in the far field is to use the Gerchberg–Saxton iterative algorithm [16, 17]. Using the data on the initial intensity distribution and knowing the point spread function, it is possible to solve a theoretical problem of phase reconstruction in the near field. However, since the algorithm is highly sensitive to intensity fluctuations, in experimental implementation the correct solution may not be found in a number of cases: The phase delay determined by the Gerchberg–Saxton algorithm does not provide the required intensity distribution in the observation plane. For this reason, we propose to present the phase delay in the form of a superposition of Zernike polynomials with subsequent iterative optimisation of their coefficients to obtain a desired focal spot shape in the observation plane.

To solve the problem of forming a specified intensity distribution in the far field, the following algorithm for calculating the phase delay was proposed:

1. The intensity distribution in the far field was specified analytically (usually, centrally symmetric).

2. The required wavefront was represented as a superposition of Zernike polynomials. The coefficients of these polynomials were determined using an iterative hill-climbing algorithm (numerical solution to the problem of obtaining a specified intensity distribution in the lens focal plane).

3. The wavefront calculated was approximated by response functions of the deformable mirror drivers. Control signals (voltages) were calculated, which were then fed to individual drivers to form the required phase.

4. The wavefront formed was analysed using a Shack–Hartmann sensor. To minimise the difference between the calculated wavefront and the real phase surface reconstructed using the adaptive mirror, a feedback system was used.

5. The intensity distribution in the observation plane was recorded using a CCD camera. The discrepancy between the obtained and required intensity distributions was compensated for using the hill-climbing algorithm by successive variation of control signals on the adaptive mirror drivers.

6. After obtaining a specified intensity distribution, the iteration algorithm was suspended, and the corresponding wavefront was measured, which was then used as a reference in the phase conjugation system to further maintain the focal spot shape in the conditions of radiation phase fluctuations.

Thus, the proposed algorithm makes it possible to form a specified intensity distribution of the focal spot and simultaneously compensate for a change in the radiation aberrations in real time. A system for the algorithm implementation should include a deformable mirror, a wavefront sensor and a CCD camera installed in the far field.

2. Deformable mirror

The key element of any adaptive optical system is a wavefront corrector, for example, a flexible mirror. In this paper, we employed a wavefront corrector based on a semipassive bimorph piezoelectric element [18, 19]. The main advantage of this type of mirror is that it perfectly reproduces lower-order aberrations. A conventional bimorph mirror consists of a relatively thick glass substrate, rigidly glued to a flat, thin piezoceramic disk. By applying an electrical signal to the electrodes, it is possible, due to the piezoceramic effect, to obtain a bend of the surface wavefront corrector.

Basic parameters of the deformable mirror used in this work are presented below.

Mirror type	bimorph
Active aperture diameter/mm	50
Initial surface roughness (P–V)/μm	0.5
Deformation value/μm	20
Number of electrodes	48
Range of applied voltages/V	–200…+300

3. Shack–Hartmann sensor

To analyse the wavefront of light beams, a Shack–Hartmann sensor is commonly used [11–15]. In addition, sensors of this type are increasingly used in devices for measuring the quality of optical elements [20], thus replacing conventional interferometers [21].

The operation principle of a sensor is that, with the use of a microlens raster (lenslet), an incident wavefront is divided into separate sections, within which the local slope is considered constant. The microlens raster represents a thin plate with a pattern of microlenses etched on its surface. Each lens forms its own focal spot in the receiver plane (usually CCD or CMOS camera). Depending on the wavefront slope, the focal spots are displaced by a certain distance relative to the initial location. By analysing the displacements over the entire aperture of the beam, it is possible to calculate the local wavefront slopes in the region of each element of the microlens raster, and to reconstruct through them the entire phase surface structure.

The camera for wavefront recording, as a rule, is selected in accordance with the requirements for speed and resolution of the system. Below the main parameters of the Shack–Hartmann sensor are represented.

Sensor type	CMOS
Sensor size/inch	1/3
Sensor real size/mm	4.8 × 3.6
Microlens raster focus/mm	3.2
Distance between microlenses/mm	0.136

4. Simulation and experimental results

Before the experiments, we simulated numerically the system operation intended for the formation of the far-field radiation. It was assumed that the intensity distribution $I_{\text{sim}}(x, y)$ is constant throughout the aperture, and the phase $\varphi(x, y)$ is plane. In calculating the intensity distribution in the lens focal region, we used the Fraunhofer diffraction integral [22]:

$$I_{\text{sim}}(k_x, k_y, a) = \left| \iint \mathrm{d}x\mathrm{d}y \sqrt{I(x,y)} \exp\left[\frac{2\pi \mathrm{i}\varphi(x,y,a)}{\lambda}\right] \exp[-2\pi \mathrm{i}(k_x x + k_y y)] \right|^2, \quad (1)$$

where $k_x = x/(f\lambda)$, $k_y = y/(f\lambda)$; (x, y) are the coordinates of a point in space; λ is the wavelength; f is the focal length of the microlens raster lenses; and a is a set of coefficients for Zernike polynomials.

The method for forming the intensity distribution $I_{\text{des}}(x, y)$ was numerically tested for two types of distributions: 1) an

doughnut distribution, which in the two-dimensional case has the form

$$I_{\text{des}}(x,y) = \exp\left\{\frac{-[\sqrt{(x^2+y^2)} - H/2]^2}{D^2/8}\right\} + \exp\left\{\frac{-[\sqrt{(x^2+y^2)} + H/2]^2}{D^2/8}\right\}, \quad (2)$$

where D is the ring diameter and H is the distance between the ring maxima, and 2) a super-Gaussian distribution:

$$I_{\text{des}}(x,y) = \exp\left[-2\left(\frac{x^2+y^2}{R^2}\right)^N\right], \quad (3)$$

where R is the input beam radius and N is the order of the super-Gaussian distribution.

According to the technique presented above, in order to form a specified intensity distribution, the radiation wavefront incident on the focusing lens was represented as a superposition of centrally symmetric Zernike polynomials [23]. The coefficients for these polynomials were calculated using the hill-climbing method. Their values were found by minimising the functional

$$\Phi = \sum\sum \left| I_{\text{des}}(x,y) - I_{\text{sim}}(x,y,a) \right|^2, \quad (4)$$

where the intensity distribution was calculated by formula (1).

Using the calculated coefficients for polynomials, a phase surface was determined, which was then approximated by the experimentally measured response functions of the bimorph mirror. To this end, in accordance with the calculated Zernike polynomials, an array of displacements of the hartmanogram's focal spots relative to the reference positions (corresponding to the planar phase of the radiation) was found:

$$\sum_{p=1}^{NP} a_p \frac{\partial Z_p(x_k,y_k)}{\partial x} = \frac{1}{f} S_x(x_k,y_k),$$
$$\sum_{p=1}^{NP} a_p \frac{\partial Z_p(x_k,y_k)}{\partial y} = \frac{1}{f} S_y(x_k,y_k), \quad (5)$$

where a_p is the coefficient of the Zernike polynomial with the number $p = 1,\ldots,NP$; NP is the number of polynomials; $\partial Z_p(x_k, y_k)/\partial x$ is the polynomial's derivative with number p along the X axis at point (x_k, y_k); $\partial Z_p(x_k, y_k)/\partial y$ is the polynomial's derivative with number p along the Y axis at point (x_k, y_k); f is the lenslet focus; $S_x(x_k, y_k)$ is the focal spot displacement with number k along the X axis; and $S_x(x_k, y_k)$ is the focal spot displacement with number k along the S_y axis.

With the use of the displacements obtained, a set of voltages have been found to minimise the functional:

$$\min |\boldsymbol{S} - \boldsymbol{bu}|^2, \quad (6)$$

where $\boldsymbol{S}$ is the array of displacements found by means of (5) and containing the displacements along both axes; $\boldsymbol{b}$ is a matrix of the response functions of the deformable mirror; and $\boldsymbol{u}$ is the required vector of voltages to be applied to the mirror electrodes. Then, in accordance with the voltages found, we have determined the displacement vector [according to (6)], the phase surface [according to (5)], and the intensity distribution in the lens focal plane [according to (1)], which should be obtained by applying the calculated voltages to the mirror control elements.

To verify the correctness of this method, an experimental setup was assembled (Fig. 2). The radiation of a 635-nm diode laser was expanded with a telescope to 50 mm and fell on a flexible bimorph mirror. Part of the laser beam was directed to the focusing lens and was further analysed by a CCD camera. The other part of the radiation, after passing through a demagnifying telescope, fell onto the Shack–Hartmann wavefront sensor, which was used to measure the response functions of the bimorph mirror. Then, the pre-calculated wavefront, which was required to obtain a specified intensity distribution in the observation plane, was reproduced by a bimorph mirror (using a closed adaptive system and Shack–Hartmann sensor data). The thus formed radiation was recorded with a CCD camera.

As was to be expected, due to various unaccounted aberrations, alignment inaccuracies and other noise factors, the resulting focal spot turned out different from that calculated analytically with the use of the found set of control voltages. However, this result served as a good initial approximation for the application of the hill-climbing algorithm in order to optimise the focal spot with subsequent quick achievement of the specified intensity distribution.

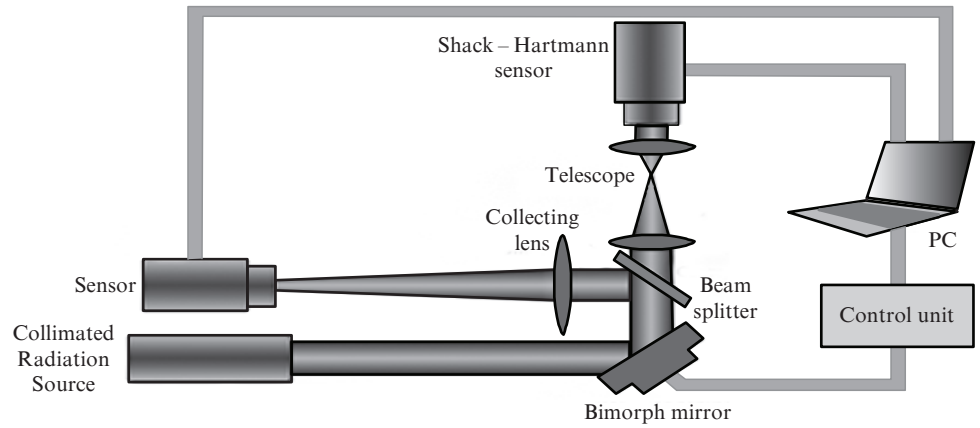

Figure 2. Scheme of an adaptive optical system for the formation of a specified intensity distribution in the far field.

A criterion for the hill-climbing algorithm to optimise the experimentally obtained intensity distribution was minimisation of the sum of squares of the differences between the required intensities and those obtained with the use of the camera:

$$\Phi_1 = \sum\sum \left| I_{\text{des}}(x,y) - I_{\text{real}}(x,y) \right|^2, \quad (7)$$

where $I_{\text{real}}(x, y)$ is the far-zone intensity at point (x, y).

Numerical modelling of radiation propagation and its focusing into an assigned centrally symmetric intensity distribution has shown that as many as three centrally symmetric Zernike polynomials describing defocusing (Z3) and spherical aberrations (Z8 and Z15) would suffice to obtain a satisfactory result. According to calculations, the symmetric higher-order wavefront aberrations are virtually zero and do not affect the focal spot shape in the far field, and therefore can be excluded from consideration.

As an example of the proposed method application, Fig. 3 illustrates the results of a doughnut intensity distribution formation. Figure 3a shows an initial, experimentally measured, focal spot, and Fig. 3b presents a specified intensity distribution; the calculated value of the beam phase corresponds to the following set of the coefficients for Zernike polynomials: 0.53 (Z3), –0.18 (Z8) and –0.2 (Z15). Figure 3c shows the result of the formation of a doughnut intensity distribution using the approximation of an ideal phase by a real bimorph mirror. High sensitivity of the mirror to the voltage changes (which in this case is a disadvantage of the flexible mirror used) along with the nonlinearity of the response of electrodes (hysteresis) did not allow us to achieve the best results using the phase conjugation algorithm. In this case, the absence of symmetry in the resulting focal spot is clearly visible. Figure 3d demonstrates the result of using the hill-climbing method for obtaining a doughnut intensity distribution.

Figure 3. Results of the formation of a doughnut intensity distribution: (a) initial intensity distribution; (b) required intensity distribution; (c) surface recorded by the CCD camera after the phase surface restoration by the deformable mirror; (d) focal spot obtained after the use of the hill-climbing method.

Figure 4 presents the results of the formation of a super-Gaussian intensity distribution. Figure 4a shows the initial focal spot, and Fig. 4b – the required super-Gaussian intensity distribution. The calculated value of the beam phase corresponds to the following set of the coefficients for Zernike polynomials: 0.53 (Z3), –0.14 (Z8) and –0.20 (Z15). Figure 4c demonstrates the result of the formation of a super-Gaussian distribution using the phase conjugation method. As in the case of the doughnut intensity distribution formation, the resulting spot is asymmetric. Figure 4d illustrates the intensity distribution obtained after applying the hill-climbing method.

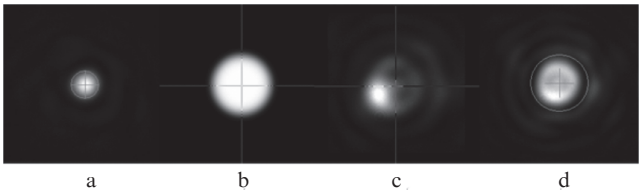

Figure 4. Results of the formation of a super-Gaussian intensity distribution: (a) initial intensity distribution; (b) required intensity distribution; (c) surface recorded by the CCD camera after the phase surface restoration by the deformable mirror; (d) focal spot obtained after the use of the hill-climbing method.

It should be noted that for both doughnut and super-Gaussian intensity distributions, the energy concentration in the required region was about 75%.

After obtaining a focal spot of the required shape, the image from the Shack–Hartmann wavefront sensor was recorded as a reference image for the adaptive optical system. With the use of this reference image, the phase conjugation mechanism was implemented, which allows a given far-zone intensity distribution to be simulated in real time.

Thus, we have shown that a bimorph mirror is an instrument which allows the laser beam position to be controlled and its focal spot to be modified. We have presented a fairly efficient and effective technique for the formation of a specified intensity distribution by two sensors: one for measuring the phase (Shack–Hartmann sensor), and the other for analysing the intensity distribution (a CCD camera located in the lens focal plane). As a result, we have obtained doughnut and super-Gaussian intensity distributions in the lens focal plane with a radiation energy concentration of 75%.

Acknowledgements. The work was supported by the Russian Foundation for Basic Research (Scientific Project Nos 16-07-01097a, 15-08-07986 a).

References

1. Laskin A., Laskin V. *Proc. SPIE*, **8236**, 82360D (2015).
2. Möhl A., Fuchs U. *Adv. Opt. Technol.*, **5** (3), 201 (2012).
3. Miklyaev Yu.V., Krasnaberski A., Ivanenko M., Mikhailov A., Imgrunt W., Aschke L., Lissotschenko V.N. *Proc. SPIE*, **7913**, 79130B (2011).
4. Sisakyan I.N., Soifer V.A. *Komp'yuternaya Optika*, **1**, 5 (1989).
5. Koronkevich V.P., Lenkova G.A., Mikhaltseva I.A., et al. *Avtometriya*, **1**, 4 (1985).
6. Akahane Y., Ma J., Fukuda Y., Aoyama M., Kiriyama H., Yamakawa K., Sheldakova J.V., Kudryashov A.V. *Rev. Sci. Instrum.*, **77** (2), 023102 (2006).
7. Boyko O., Planchon Th.A., Mercere P., Valentin C., Balcou Ph. *Opt. Commun.*, **246**, 131 (2005).
8. Himmelblau D.M. *Applied Nonlinear Programming* (New York: McGraw-Hill, 1972).
9. Glebov N.I., Kochetov Yu.A., Plyasunov A.V. *Metody optimizatsii (uchebnoe posobie)* (Optimisation Methods (A Textbook)) (Novosibirsk: Izd. Novosibirsk. Univer., 2000).
10. Glushkov V.M. *Vvedenie v ASU* (Introduction to Automated Control Systems) (Kiev: Tekhnika, 1974).
11. Neal D.R., Copland J., Neal D. *Proc. SPIE*, **4779**, 148 (2002).
12. Makenova N., Kanev F., Lukin V. *Proc. SPIE*, **5026**, 190 (2003).
13. Starikov F.A., Kochemasov G.G., Kulikov S.M., Manachinsky A.N., Maslov N.V., Ogorodnikov A.V., Sukharev S.A., Aksenov V.P., Izmailov I.V., Kanev F.Yu., Atuchin V.V., Soldatenkov I.S. *Opt. Lett.*, **32** (16), 2291 (2007).
14. Kudryashov A.V., Samarkin V.V., Sheldakova Yu.V., Aleksandrov A.G. *Avtometriya*, **48** (2), 52 (2012).

15. Kudryashov A.V., Samarkin V.V., Sheldakova Y.V., Aleksandrov A.G. *Optoelectron. Instrum. Data Proc*., **48** (2), 153 (2012).
16. Gerchberg R.W., Saxton W.O. *Optik*, **35**, 227 (1972).
17. Ilyina I.V., Cherezova T.Yu., Kudryashov A.V. *Proc. SPIE*, **6452**, 64520C (2007).
18. Samarkin V., Alexandrov A., Borsoni G., Jitsuno T., Romanov P., Rukosuev A., Kudryashov A. *High Power Laser Sci. Eng.*, **4**, e4 (2016).
19. Kudryashov A., Samarkin V., Aleksandrov A., Borsoni G., Jitsuno T., Romanov P., Sheldakova J. *Proc. SPIE*, **18**, 97271I (2016).
20. Nikitin A., Sheldakova J., Kudryashov A., Borsoni G., Denisov D., Karasik V., Sakharov A. *Proc. SPIE*, **9754**, 97540K (2016).
21. Vitrichenko E.A., Lukin V.P., Pushnoy L.A., Tartakovsky V.A. *Problemy opticheskogo kontrolya* (Optical Control Problems) (Novosibirsk: Nauka, 1990).
22. Goodman J. *Introduction to Fourier Optics* (New York: W.H. Freeman & Co Ltd, 2004; Moscow: Mir, 1970).
23. Noll R.J. *J. Opt. Soc. Am*., **66** (3), 207 (1976).